Water Science & Technology

Water Science & Technology Vol 87 No 4, 879 doi: 10.2166/wst.2023.043

Study on low temperature plasma combined with AC/Mn + TiO_2–Al_2O_3 catalytic treatment of sewage-containing polyacrylamide

Xiaobing Wang*, Fengwei Guan, Zhigang Huang, Hao He, Lu Wang and Kaifeng Li

School of Petroleum Engineering and Natural Gas Engineering, Changzhou University, Changzhou 213016, China
*Corresponding author. E-mail: wangxb@cczu.edu.cn

ABSTRACT

With the introduction of tertiary oil recovery technology, polymer oil drive technology has effectively improved the recovery rate of crude oil, but the resulting oilfield wastewater-containing polyacrylamide (PAM) is viscous and complex in composition, which brings difficulties to wastewater treatment. The treatment of this kind of wastewater has become an urgent problem to be solved, and the removal of PAM is the key. In this paper, a dielectric barrier discharge (DBD) co-catalyst was used to treat PAM-containing solutions to investigate the effect of different catalytic reaction systems on the degradation of PAM. The morphological changes of the PAM solution before and after the reaction were also studied by the environmental electron microscope scanner (ESEM), and the information of the functional groups in the solution before and after the reaction was studied by infrared spectroscopy analysis of the PAM solution. The degradation rate rose by 26.3% in comparison to that without discharge when AC/Mn + TiO_2 and Al_2O_3 were combined and catalyzed at a mass ratio of 2:1 and a discharge period of 300 min. The degradation rate rose by 19.3 and 6.8%, respectively, in comparison to AC/Mn + TiO_2 and Al_2O_3-catalyzed alone. It demonstrates that this catalytic system has the optimum catalytic effect.

Key words: degradation rate, low-temperature plasma, polyacrylamide, synergistic catalysis, wastewater treatment

HIGHLIGHT

- In this paper, the feasibility of low-temperature plasma generated by dielectric barrier discharge (DBD) to degrade poly-containing wastewater was studied. From the perspective of improving the degradation efficiency, a double glass DBD reactor with a water-cooling function was designed, and the effect of low-temperature plasma on the degradation rate of PAM solution under different catalyst combinations conditions was studied.

GRAPHICAL ABSTRACT

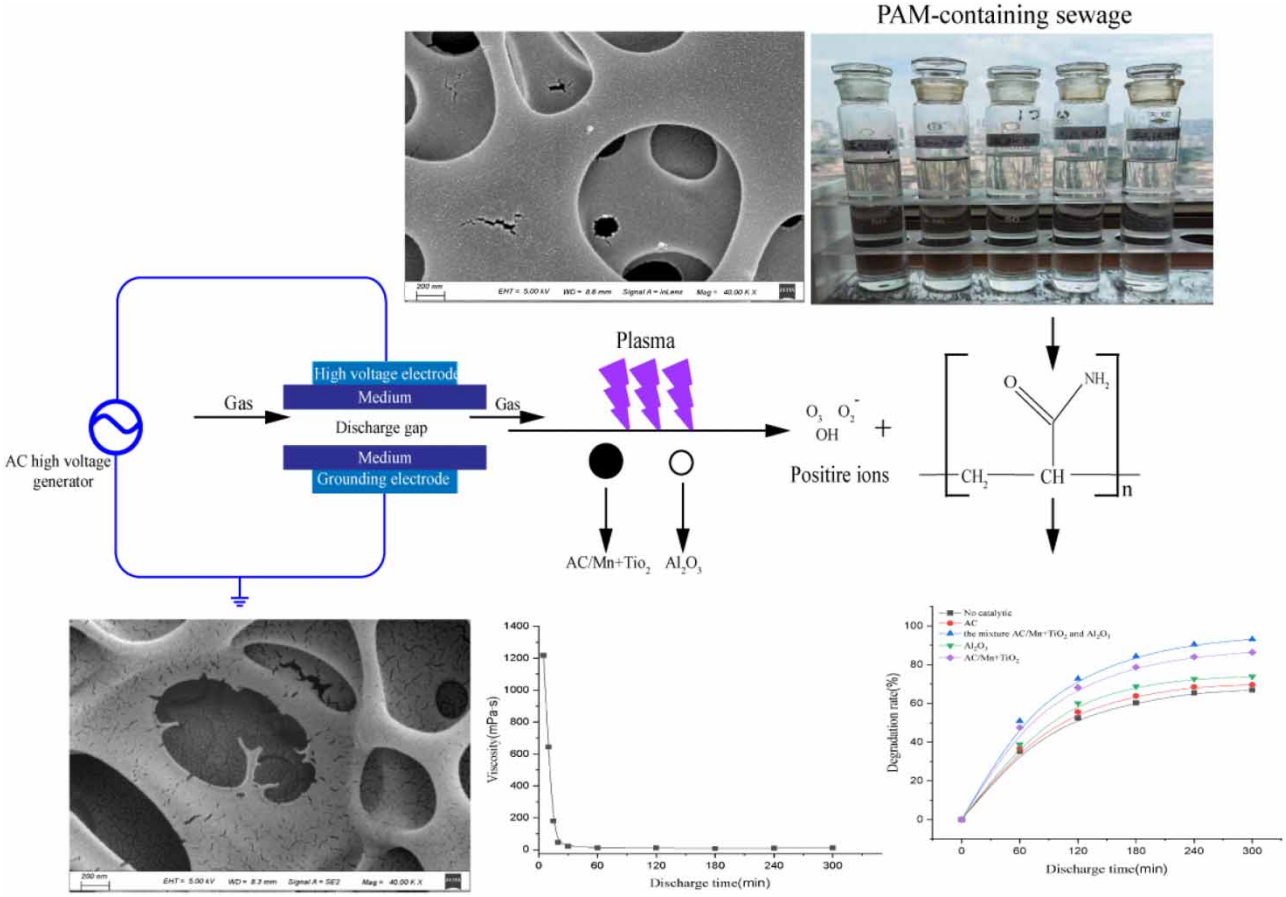

1. INTRODUCTION

The polymer flooding tertiary oil recovery technology used in oil and gas field development is effective in improving oil recovery, but it produces a large amount of wastewater-containing polymer. Polyacrylamide (PAM) is the main component of polymer-containing wastewater. The untreated polymer-containing wastewater has high emulsification and high viscosity. When it is directly discharged, it will cause great damage to the ecological environment. The technology of highly efficient treatment of polymer-containing wastewater in oil fields has become a research hotspot and a difficult problem in the field of water treatment in recent years. The existing main treatment methods are flawed (Hu *et al.* 2006; Al Momani & Örmeci 2014; Farrokhpay & Filippov 2017; Ma *et al.* 2017). The physical method removes PAM from wastewater through adsorption, extraction, membrane separation and other physical functions, but this method only transfers pollutants, which is difficult to destroy the internal structure of PAM and cannot eradicate pollutants (Zhu *et al.* 2017; Wei *et al.* 2018; Crema *et al.* 2020). The chemical method uses a large number of chemical reagents to carry out the chemical decomposition reaction with PAM to achieve sewage purification. The dosage of chemical reagents generally has the optimal concentration range. When the optimal proportion is exceeded, the excessive chemical reagent will also act as a free radical trapping agent, which will inhibit the degradation of the polymer. Excessive chemical reagents will pollute water. The comprehensive cost of the chemical method is generally high (Lu *et al.* 2012; Yin *et al.* 2017; Meng *et al.* 2018). The biological method is to decompose PAM into small molecular substances by the metabolism of microorganisms in water. Microbes have high requirements for the water environment and are easily affected by water pH and temperature. It is urgent to develop a new, efficient and economic water treatment process to solve the problem of wastewater-containing PAM (Gilbert *et al.* 2017; Zhao *et al.* 2019; Ma *et al.* 2021).

As a new advanced oxidation technology, the plasma water treatment technology can ionize the air to produce a large number of active substances only through discharge without adding any chemicals. The discharge process has physicochemical effects such as ultraviolet, ultrasonic and thermal radiation, which can effectively realize the degradation of organic pollutants. Kim *et al.* used low-temperature plasma to treat sulfamethoxazole and other antibiotics in water. All three antibiotics with the initial concentration of 50 mg/L were degraded after 20 min of discharge treatment in an oxygen medium (Kim *et al.* 2015). Sang *et al.* used plasma technology to treat 1,000 mg/L *N*,*N*-dimethylformamide solution. After 40 min, the degradation rate reached 52.2%, and TOC decreased by 35.8%, indicating that plasma can directly mineralize pollutants in wastewater (Sang *et al.* 2019). The plasma water treatment technology uses electric energy as the energy source. Compared with the traditional water treatment technology, it produces less pollution and by-products, and has good compatibility with the environment (Zhan *et al.* 2018; Guo *et al.* 2019; Xu *et al.* 2020; Berardinelli *et al.* 2021).

Due to the complex types of active particles in plasma and the diversity of organic pollutant degradation reaction paths, plasma technology has the problems of poor organic conversion selectivity and low-energy utilization efficiency in the practical application process. The reactor running at high power will also produce harmful gases such as O_3 and NO_x with high concentrations (Jiang *et al.* 2018; Qin *et al.* 2021). Researchers combined plasma technology and catalyst to solve these problems. By the synergistic effect, high treatment efficiency can be achieved at a low discharge power, energy consumption can be reduced and the problem of toxic by-products generated by low-temperature plasma at high power operation can be avoided. A variety of physicochemical effects of discharge, such as high electric field and shock wave, can clean the surface of the catalyst and help the regeneration of the catalyst, which saves the cost of water treatment (Ma *et al.* 2017). At present, the catalysts used for plasma catalytic oxidation mainly include carbon catalysts mainly based on activated carbon, photocatalysts mainly based on titanium dioxide, and other metal catalysts, metal or metal oxide catalysts supported on the support, and others (Zhou *et al.* 2016; Tang *et al.* 2017). In recent years, the research on plasma-assisted catalytic water treatment technology has also made some progress. In 2019, Ren *et al.* treated trans-ferulic acid with Fe^{2+}, Cu^{2+} and plasma. Compared with plasma treatment alone, the degradation rate increased by 10% after 15 min (Ren *et al.* 2019). Gong *et al.* used Ag_3PO_4 @ carbon fiber composite catalyst synergistic plasma system to degrade levofloxacin contaminants, and the degradation rate of levofloxacin was increased by 30%. The mineralization rate was increased by 35% in 18 min compared with the plasma alone (Gong *et al.* 2020). In 2020, Ahmadi *et al.* combined α-Fe_2O_3-TiO_2 nanocomposite catalyst and $Na_2S_2O_8$ with plasma for the treatment of dimethyl phthalate (DMP). Under optimal process conditions, the complete degradation of contaminants was achieved with a reaction time of 5.2 min (Ahmadi *et al.* 2020). In 2021, Deng *et al.* used low-temperature plasma to synergize FeO–CeO_2 for the catalytic degradation of wastewater-containing diclofenac. The degradation rate improved from 45.8 to 96.4% with the addition of the catalyst, and the synergistic coefficient of the two reached 3.731 (Deng *et al.* 2021). Tang *et al.* used plasma to synergize sodium persulfate to treat tetracycline-containing wastewater. The degradation efficiency of tetracycline increased from 30 to 70% within 5 min, and the reaction kinetic constant increased by 79.7% within 15 min, showing a good synergistic effect (Tang *et al.* 2018).

It can be seen from the above research that the addition of the catalyst has significantly improved the efficiency of plasma sewage treatment. However, the introduction of a single catalyst cannot fundamentally improve the degradation efficiency of organic pollutants. TiO_2, ZnO and other photocatalysts can only effectively use the ultraviolet light generated in the system. Al_2O_3 and other adsorbents themselves do not have excellent catalytic performance. Metal ion reagents will cause secondary pollution to water. Activated carbon and catalyst supported on activated carbon will be damaged to varying degrees during the discharge process, affecting their catalytic activity. In this paper, the PAM solution was treated by plasma technology in coordination with Al_2O_3 catalyst with high adsorption capacity and AC/Mn + TiO_2 composite photocatalyst supported on activated carbon. The effects of different catalytic reaction systems on the degradation rate of PAM solution were studied, and the best plasma synergistic catalytic reaction system was obtained, which provided a basis for the treatment of polymer-containing wastewater in industrial production.

2. EXPERIMENTAL SECTION

2.1. Reagents and equipment required for the experiment

The reagents required for the experiment are listed in Table 1, and the equipment required for the experiment is listed in Table 2.

Table 1 | List of reagents required for the experiment

Reagent name	Purity	Manufacturer
Polyacrylamide	AR	Beijing Hengju Group
Ice acetic acid	AR	Changzhou Main Chemical Co.
Sodium hypochlorite	AR	Changzhou Main Chemical Co.
Glutaraldehyde	AR	Changzhou Main Chemical Co.
Ethanol	AR	Changzhou Main Chemical Co.
Potassium bromide	AR	Changzhou Main Chemical Co.
Sodium hydroxide	AR	Hebei Shengqiang Chemical Co.
Titanium dioxide	AR	Changzhou Main Chemical Co.
Manganese oxide	AR	Changzhou Main Chemical Co.
Activated carbon granules	AR	Zibo Bell Chemical Technology Co.
Activated alumina granules	AR	Zibo Beier Chemical Technology Co.

Table 2 | Equipment required for the experiment

Instrument name	Model	Manufacturer
Plasma generator	CTP-2000K	Nanjing Suman Electronics Co., Ltd.
Contact voltage regulator	TDGC2-1	Zhenhua Transformer Manufacturing Co., Ltd.
Oscilloscope	100 m utd2102cex	Youlide Technology Co., Ltd.
Spectrophotometer	Model 722	Shanghai Jingke Industrial Co., Ltd.
Electronic balance	AR114	Shenyang Longteng Electronics Co., Ltd.
Miniature vacuum air pump	SYB71-7D	Haixun Fluid Technology Co., Ltd.
Magnetic heating agitator	JB-13	Shanghai Leici Instrument Factory
Electric blender	GZ-120WS	Lingke Electric Appliance Co., Ltd.
Thermostatic drying chamber	pH-14	Qixin Scientific Instrument Co., Ltd.
Environmental scanning electron microscope	GerminiSEM300	Zeiss Gruppe
FTIR Spectrometer	IR-2000	JingTuo Instrument Technology Co., Ltd.

2.2. Preparation of catalyst

The AC particles with a certain mass and diameter of 2 mm were weighed on an electronic balance, rinsed with deionized water and placed in dilute hydrochloric acid at a concentration of 0.1 mol/L for 12 h. The AC particles were removed and rinsed repeatedly with deionized water, then placed in sodium hydroxide at a concentration of 0.1 mol/L for 12 h. After soaking, the AC pellets were repeatedly rinsed with deionized water and dried in a drying oven at 108 °C for 24 h.

AC/Mn + TiO_2 was prepared by the powder sintering method. About 10 g of anatase TiO_2 nanopowder and 5 g of MnO nanopowder were added to 200 mL of boiling deionized water, stirred continuously and then placed in an ultrasonic environment for 2 h. After that, the powder was dried in a drying oven at 108 °C for 24 h. After drying, the powder was calcined in a resistance furnace at 400 °C for 5 h to obtain Mn/TiO_2-loaded AC particles, referred to as 'AC/Mn + TiO_2', with each AC/Mn + TiO_2 having a diameter of about 2.5 mm and a weight of about 136 mg.

2.3. Experimental process

The specific experimental process is divided into the following seven steps:

(1) A mass of 1,000 mg of PAM was separately measured using a balance and mixed with 1 L of deionized water. PAM powder was slowly poured into deionized water after stirring for 2 h and then left for 24 h.

(2) The experiment was carried out in a self-made reactor (a quartz reactor with a double-layer groove structure, a quartz reactor with the wall thickness of 3 mm, a diameter of 125 mm, the width of a cooling tank of 15 mm, the inlet and outlet diameter of air and cooling water of 5 mm, and the thickness of stainless steel electrode of 2 mm) at room temperature. About 150 mL of the configured PAM solution was poured into the discharge device, and different catalyst combinations with a fixed total mass were added. The flow rate of air is set to 0.02 m^3/s, and the flow rate of cooling water is about 8.5×10^{-6} m^3/s. The ionization atmosphere, catalyst, and solution are fully contacted and mixed using the magnetic stirrers, which are rotated at a speed of 30 rpm. At the end of the discharge, the solution was removed to detect and analyze the treatment effect. The experimental setup is shown in Figure 1.

(3) According to the standard Q/SYDQ0928-2017, the absorbance of PAM solution was measured, and the absorbance and the solution concentration standard curve were drawn, as shown in Figure 2. The fitting equation of the standard curve is as follows:

$$y = (1284.69x - 105.86)N \tag{1}$$

where y is the PAM solution concentration, x is the absorbance, and N is the dilution of the solution.

(4) The absorbance of PAM solution after the reaction was measured according to the standard, and the concentration of PAM solution after the discharge was obtained by substituting it into Equation (1), and the degradation rate was calculated:

$$\text{Degradation rate} \quad \eta(\%) = \frac{(C_0 - C)}{C_0} \times 100\% \tag{2}$$

where C_0 is the PAM concentration before the discharge and C is the PAM concentration after the discharge.

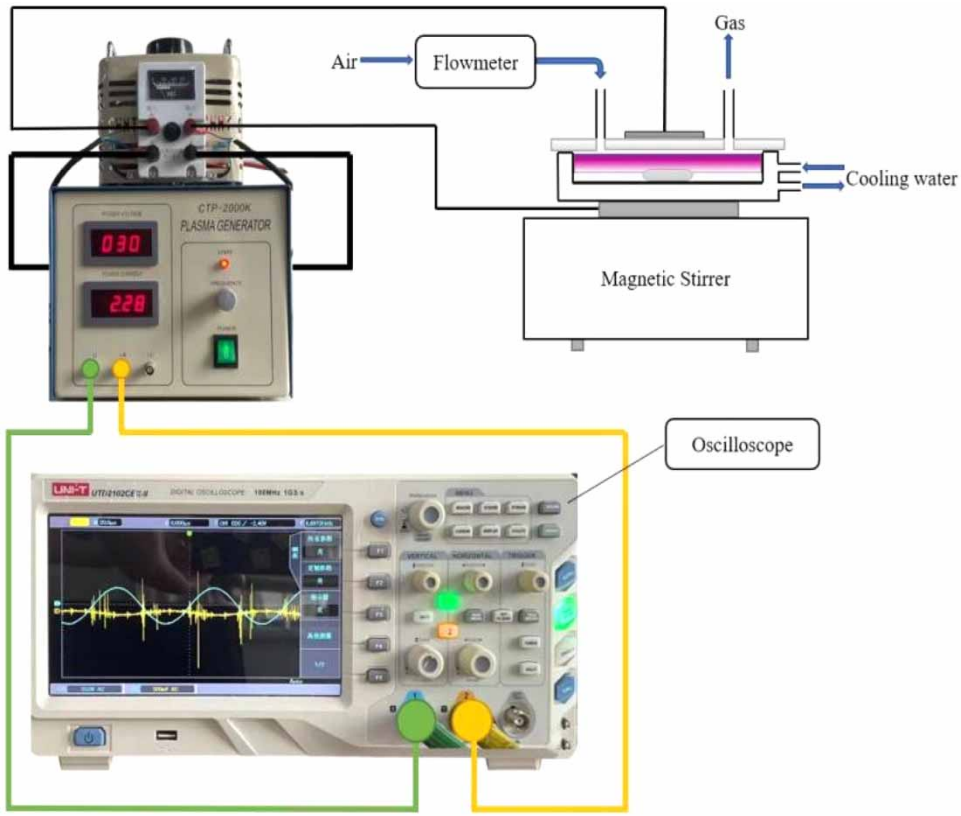

Figure 1 | Diagram of the experimental setup.

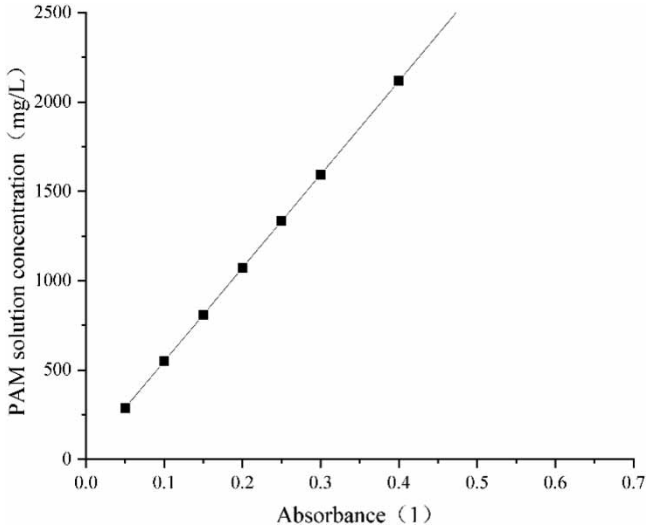

Figure 2 | Standard curves.

(5) A small amount of solution was selected, a suitable viscometer rotor was selected and the solution viscosity was measured with a digital viscometer.
(6) The prepared PAM hydrogel was laid into a thin layer, fixed with 2% glutaraldehyde for more than 4 h, then cleaned with PBS (0.1 mol/L, pH 7.2), dehydrated by ethanol with different concentration gradients, and dried, sticky and sprayed in a LEICA CPD300 automatic critical point dryer. Finally, they were observed and photographed under a GerminiSEM300 field emission scanning electron microscope.
(7) The PAM solution before and after discharge was placed in a constant temperature drying oven at 95 °C to dry into powder, and 200 mg of KBr powder and 1 mg of dried PAM powder were fully mixed by mortar and placed in a tablet pressing mold. The pressure of the tablet pressing machine was set at 8 T/cm^2, and the tablet pressing time was 1–2 min. After the tablet pressing was completed, the tablet was placed in the FTIR test frame for measurement.

3. EXPERIMENT RESULT AND DISCUSSION

3.1. Effect of different catalytic reaction systems on the degradation rate of PAM

Under the discharge voltage of 18 kV, the frequency of 10 kHz and the airflow rate of 0.02 m^3/s, 150 mL of 1,000 mg/L PAM solution and different catalyst combinations were used for catalytic degradation experiments. The amount of catalyst was both 816 mg, and the mass ratio of AC/Mn + TiO_2 and Al_2O_3 mixture was 1:1. The absorbance was measured according to the standard and substituted into the formula to obtain the degradation rate of PAM solution before and after discharge, and the best catalytic combination condition was obtained by comparison. The relationship between PAM solution degradation rate and discharge time under different catalytic reaction systems is shown in Figure 3.

Figure 3 shows the effect of each catalytic reaction system on the PAM degradation rate and compares with the discharge treatment alone. It can be seen from the figure that the use of catalyst significantly improves the degradation rate of PAM, and it increases with the increase of discharge time. The degrading effect of AC/Mn + TiO_2 catalytic treatment is observed to be superior to that of AC catalytic treatment alone. With a reaction time of 300 min using the catalyst of AC/Mn + TiO_2, the PAM degradation rate reached 88.1%, which was 12.3% higher than with catalysis of AC, and 13% higher than with no catalyst. This is due to photons being generated during the discharge process, which will induce TiO_2 to generate holes to attract the electrons of H_2O, causing H_2O to lose electrons and form hydroxyl ·OH. The extremely strong oxidation of ·OH will attack the electron cloud on the molecular chain of PAM, destroying its molecular structure, so as to split the macromolecular PAM into small molecular substances. At the same time, manganese ions can inhibit the electron-hole recombination of TiO_2 and improve the photon utilization rate, and the AC particles have a large surface area and increase the contact area to further promote catalysis. It can be seen that AC/Mn + TiO_2 has a good catalytic effect on plasma degradation.

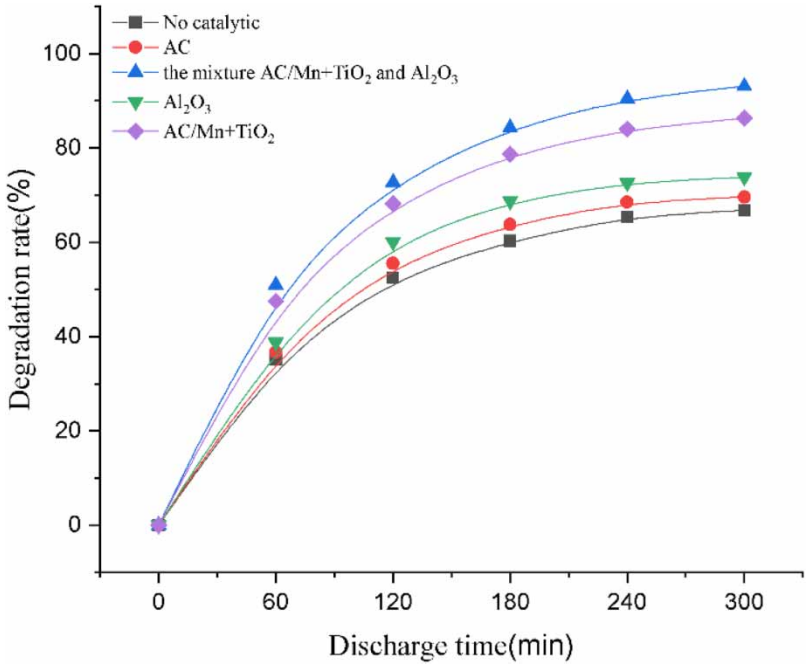

Figure 3 | Relationship between the degradation rate and the discharge time of PAM solution in different catalytic systems.

It can be seen from the figure that the adsorption of Al_2O_3 has a good auxiliary catalytic effect on the degradation of organic matter in the solution, and the PAM degradation rate is 79.3% within 300 min, which is 12.5% higher than that of the single discharge treatment. In the catalytic process, the active point on the surface of Al_2O_3 can directly react with the organic matter in the solution and produce a chelate, which is more prone to be attacked by free radicals and decomposed rapidly. When the degradation product is separated from the surface of alumina, the active point can recover and reabsorb the organic matter in the sewage to produce a new chelate, which further improves the degradation rate.

When the PAM solution was treated with AC/Mn + TiO_2 and Al_2O_3, the degradation rate reached 95.1% when the reaction reached 300 min, which was 28.3% higher than that of the single discharge treatment, and the degradation rate was also improved compared with various catalysts. This is because Al_2O_3 on the surface of AC/Mn + TiO_2 increases the catalytic effect of TiO_2. The active particles and PAM molecules generated during the discharge reaction can reach or adsorb and enrich on the surface of Al_2O_3, dramatically enhancing the effective collision probability between active particles, PAM and TiO_2, and thus significantly improving the degradation rate.

Therefore, it can be concluded that using the mixture of AC/Mn + TiO_2 and Al_2O_3 to catalyze the treatment of PAM solution not only utilizes the photocatalytic property of TiO_2 and the adsorption property of Al_2O_3, but Al_2O_3 also widens the energy gap of TiO_2 photocatalyst, so that the electron-hole has stronger redox ability and stronger photocatalytic ability, which effectively improves the degradation rate and is better than other catalytic reaction systems.

3.2. Effect of different mass ratio of AC/Mn + TiO_2 and Al_2O_3 mixed catalyst on PAM degradation rate

On this basis, we further investigated the catalytic degradation of PAM by discharging 150 mL of 1,000 mg/L PAM solution at a discharge voltage of 18 kV, a frequency of 10 kHz, an airflow rate of 0.02 m^3/s and a fixed total mass of 816 mg of AC/Mn + TiO_2 and Al_2O_3 mixed catalyst. The effect of different mass ratios of AC/Mn + TiO_2 and Al_2O_3 catalysts on the degradation rate of PAM was investigated. The specific relationship is shown below.

It is obvious from Figure 4 that the degradation rate of AC/Mn + TiO_2 to Al_2O_3 with a mass ratio of 2:1 for PAM is significantly better than other ratios as the discharge time increases, and the degradation rate of PAM reaches the highest at 300 min as the discharge time increases. The degradation rate is at a low level for the mass ratio of AC/Mn + TiO_2 to Al_2O_3 of 1:4, 1:3 and 1:2 in Figure 4. Too high a content of Al_2O_3 is not uniformly dispersed on the surface of TiO_2, which tends to form a composite center of photogenerated carriers and decreases the photocatalytic activity, while too low a content of TiO_2 results

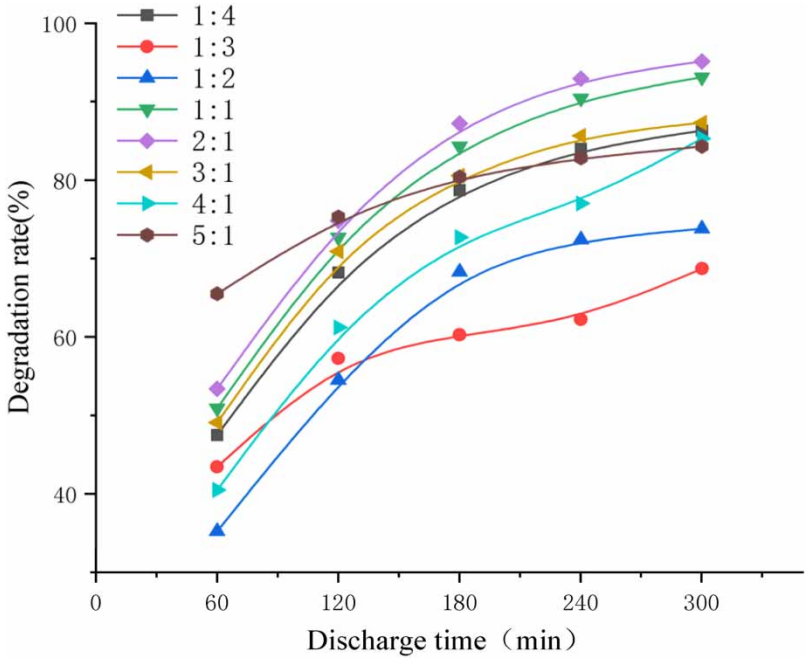

Figure 4 | Plots of degradation rates for different mass ratios and PAM solutions.

in a low yield of electron-hole, which also leads to a decrease in photocatalytic activity. The degradation rates at 60 min of discharge time were relatively high for the mass ratios of AC/Mn + TiO_2 to Al_2O_3 of 3:1, 4:1 and 5:1 in the figure, probably because the photocatalytic performance was given full play due to the high mass of TiO_2, but with time, the mass of Al_2O_3 in the solution was too low, which was not conducive to the enrichment of particles in the solution and thus affected the performance of photocatalysis, so the degradation rates at 60 min of discharge The degradation rate at 300 min was decreased to a larger extent compared with the catalyst mass ratio of 2:1.

In summary, it can be seen that the low-temperature plasma-catalyzed reaction system with a 2:1 mass ratio of AC/Mn + TiO_2 to Al_2O_3 is optimal for the degradation of PAM when the total mass of mixed catalysts in the solution is certain.

3.3. Viscosity analysis

The effect of the reaction system on the viscosity of the PAM solution was investigated at an optimum catalyst mass ratio with a discharge voltage of 18 kV, a frequency of 10 kHz and an airflow rate of 0.02 m^3/s, as shown in Figure 5.

The figure shows that the viscosity decreased by 99.06% in the first 30 min of the reaction from 1,214 to 11.4 mPa·s. The active particle bombardment generated a substantial alteration in the molecular structure of the PAM, resulting in a considerable drop in viscosity. The viscosity was maintained at a low level after 30 min. The effect of the low-temperature plasma catalytic reaction system on the viscosity of the PAM solution was mainly concentrated in the first 60 min, and it can be seen that the degradation also has a very high viscosity reduction efficiency, which aids in wastewater treatment.

3.4. Composition analysis of PAM solution before and after the reaction

3.4.1. ESEM analysis

The PAM solutions before and after the catalytic treatment with low-temperature plasma combined with AC/Mn + TiO_2 and Al_2O_3 were analyzed by environmental scanning electron microscopy.

It can be seen from Figure 6 that the structure of PAM did not change significantly when the reaction reached 20 min, but the structure began to change when the reaction reached 30 min, because the concentration of the experimentally configured solution was slightly higher, so the decomposition process of PAM was slower, and when the reaction proceeded to 45 min, PAM began to gradually cleave and become acrylamide monomer, acrylic acid and other substances.

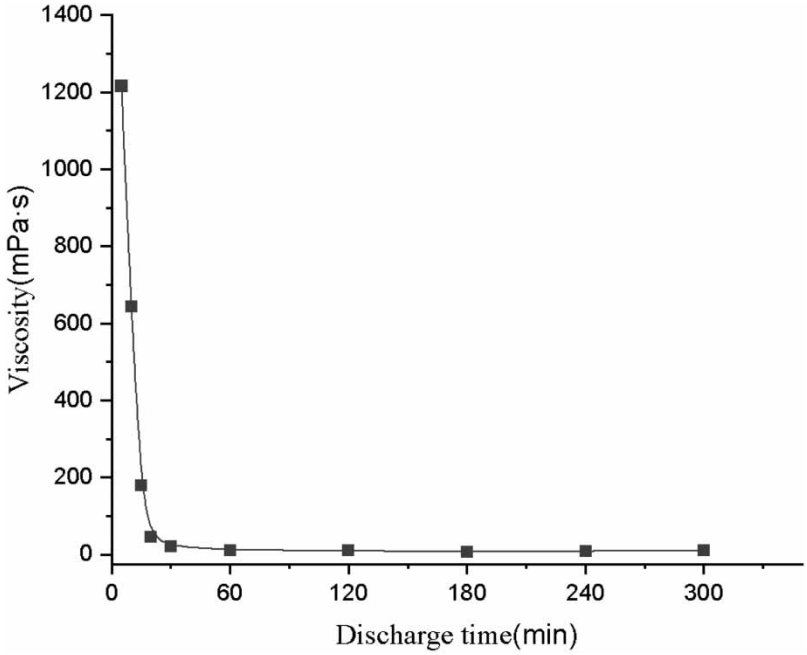

Figure 5 | Plot of viscosity as a function of time in PAM solution.

3.4.2. Infrared spectrum analysis

Infrared spectroscopy allows the composition of functional groups and groups in the solution before and after the reaction to be specifically derived, and thus the specific composition of the substance can be inferred. Figure 7 shows the IR spectra at various time periods after catalytic treatment of the PAM solution.

As can be seen from Figure 7, the absorption peaks at 3,332.67 and 3,142.81 cm^{-1} are narrower in the peak region (3,700–2,500 cm^{-1}) and are not consistent with the O–H stretching vibration. The absorption peaks at 2,895.79 cm^{-1} are C–H stretching vibrations of saturated hydrocarbon groups, and the presence of amide groups can be presumed.

In the peak region (1,900–1,500 cm^{-1}), there is a strong absorption peak at 1,633.13 cm^{-1}, which is inferred to be a C = O stretching vibration, and in the peak region (1,500–600 cm^{-1}), there is a more obvious absorption that can be judged as the characteristic absorption peaks of C–N in the primary amide. The peak region (1,250–1,000 cm^{-1}) shows a characteristic peak of 1,108.83 cm^{-1}, which can be judged as a stretching vibration of C–O in the compound.

In the plot of the reaction for 60 min, the products had absorption peaks at 3,426.57, 2,938.05, 2,322.83, 1,629.23 and 1,374.13 cm^{-1}. From the infrared plot, it can be seen that the characteristic absorption region (3,650–3,200 cm^{-1}) in the region of 3,426.57 cm^{-1} was the free O–H. The absorption peak at 2,322.83 cm^{-1} was for the lactam group (free), the absorption peak at 1,629.23 cm^{-1} was for the C = O stretching vibration and the absorption peak at 1,374.13 cm^{-1} was for the stretching vibration of C–N. The characteristic absorption peak for the stretching vibration of N–H. The absorption peak of the carbonyl group at 1,629.23 cm^{-1} is weaker and broader, indicating that the PAM may have been oxidized to aldehydes and carboxylic acids. It can be presumed that the products of PAM degradation are mainly acrylic acid and acrylamide.

The two main peak areas changed significantly from 60 to 120 min and no longer changed significantly from 120 to 300 min.

The IR spectrum at 300 min showed that there were only three absorption peaks 3,471.87, 1,649.62 and 1,385.27 cm^{-1}, the absorption peak at 3,471.87 cm^{-1} had obvious hydroxide characteristics, indicating that there was a large amount of H_2O to mask the N–H bond stretching vibration peak, 1,649.62 and 1,385.27 cm^{-1} were in the same order. The presence of carboxyl groups in the solution can still be inferred from 1,649.62 and 1,385.27 cm^{-1}, which also indirectly indicates that the small organic acids and acrylamide were further degraded to small inorganic molecules.

In summary, we can consider using this system when dealing with PAM in water that is not deionized or has more complex matrices and has been disturbed by many impurities and ions, and inadequate degradation of organic matter. Acrylamide monomer, propionamide, acetamide, acetic acid, acrylic acid and other substances will be formed in water. The free radicals

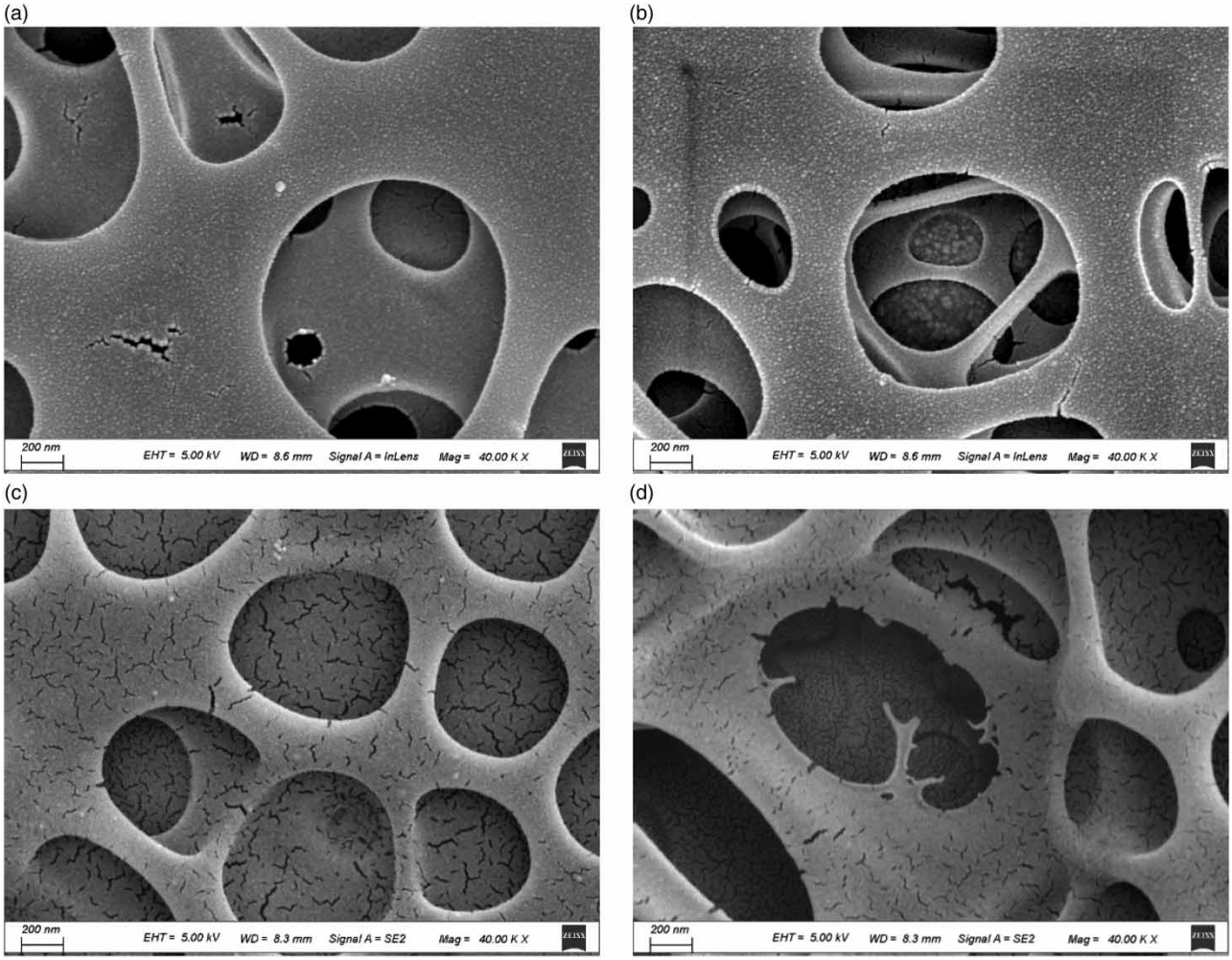

Figure 6 | ESEM plots for each time period. (a) Reaction time for 0 min. (b) Reaction time for 10 min. (c) Reaction time for 30 min. (d) Reaction time for 45 min.

produced by air discharge are transferred to the aqueous phase and react with water molecules to form various acidic substances. With the prolongation of discharge treatment time, most of the organic matter was completely mineralized to form inorganic matter such as water and carbon dioxide.

4. CONCLUSION

In this paper, the PAM solution was treated by dielectric barrier discharge (DBD) producing plasma co-catalyst, and the effect of different catalyst reaction systems on the degradation rate of PAM solution was studied. On this basis, the effect of different AC/Mn + TiO_2 and Al_2O_3 mass ratio on the degradation rate of PAM solution was studied when the total mass of the catalyst was constant. Finally, the PAM solution before and after the reaction was characterized and analyzed. The following conclusions were obtained:

(1) The hybrid catalytic discharge process of AC/Mn + TiO_2 and Al_2O_3 releases photons, which excite TiO_2 to generate holes and promote the formation of hydroxyl radical ·OH. Meanwhile, Al_2O_3 can inhibit TiO_2 electron-hole complexation, improve photon utilization and adsorb active particles and reactants, which makes this catalytic reaction system more effective compared with other reaction systems.
(2) From the comparison experiments, it was found that when the total mass of the mixed catalysts was fixed, the best degradation effect was obtained when the mass ratio of AC/Mn + TiO_2 to Al_2O_3 in the solution was 2:1 and both were better than each catalyst alone.

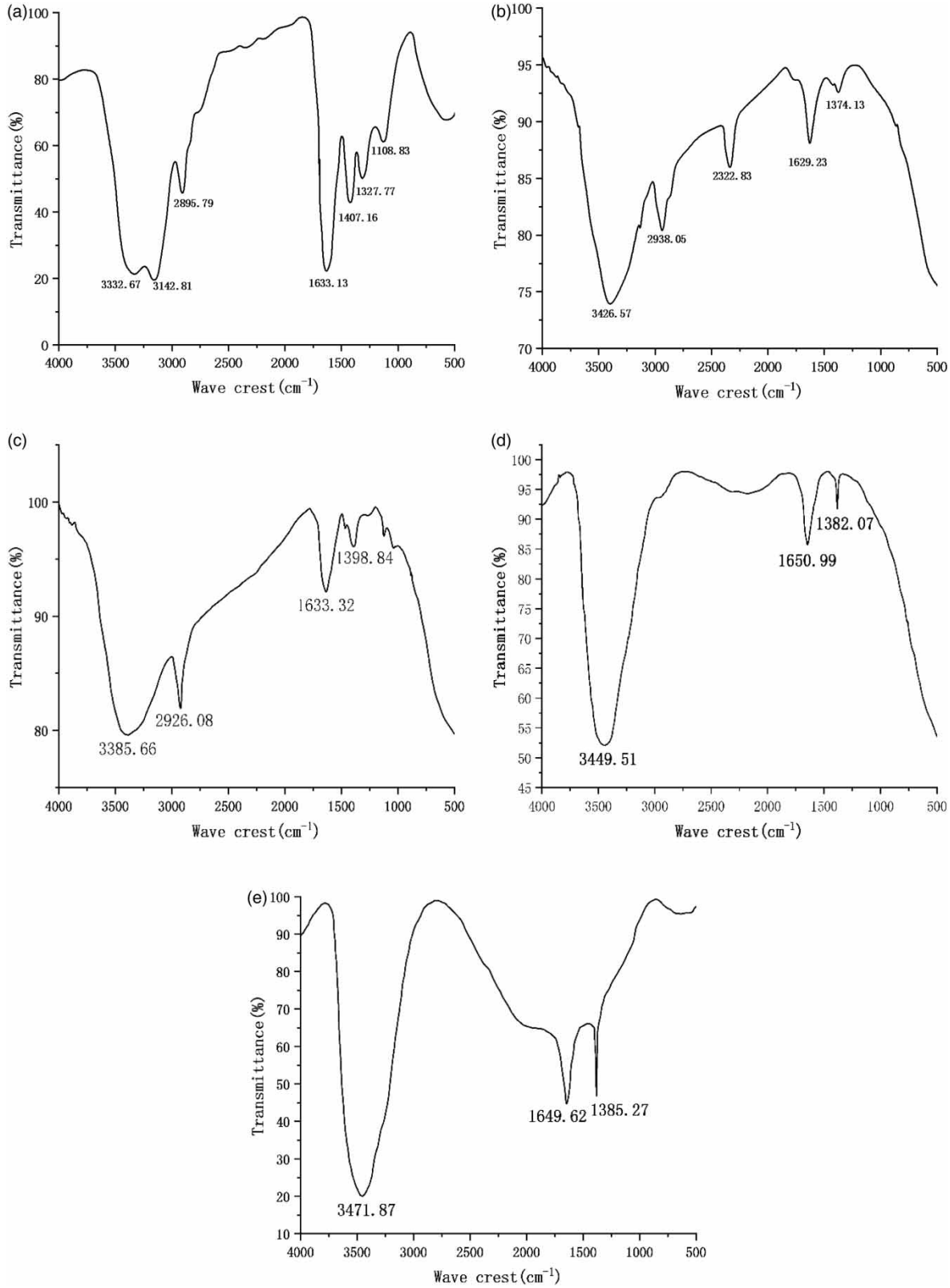

Figure 7 | IR spectra of the solution before and after the reaction. (a) Reaction time for 0 min. (b) Reaction time for 60 min. (c) Reaction time for 120 min. (d) Reaction time for 180 min. (e) Reaction time for 300 min.

(3) The low-temperature plasma catalytic degradation treatment of PAM-containing solutions reduced their viscosity by 99.06% in the first 30 min, as tested by a viscometer.
(4) As shown by ESEM and FTIR, the active components generated by the discharge firstly attack the carbon double bond, the hydroxyl group and the amino group of PAM to break the long-chain PAM to form short-chain PAM and gradually produce acrylamide and acrylic acid. The further reaction can degrade small molecules of organic matter to water and other inorganic substances.

ACKNOWLEDGEMENT

This work was jointly supported by the Open Project of the Key Laboratory of Enhanced Oil and Gas Recovery of the Ministry of Education (NEPU-EOR-2021-01).

DATA AVAILABILITY STATEMENT

All relevant data are included in the paper or its Supplementary Information.

CONFLICT OF INTEREST

The authors declare there is no conflict.

REFERENCES

Ahmadi, E., Shokri, B., Mesdaghinia, A., Nabizadeh, R., Khani, M. R., Yousefzadeh, S., Salehi, M. & Yaghmaeian, K. 2020 Synergistic effects of alpha-Fe_2O_3–TiO_2 and $Na_2S_2O_8$ on the performance of a non-thermal plasma reactor as a novel catalytic oxidation process for dimethyl phthalate degradation. *Separation and Purification Technology* **250**. https://doi.org/10.1016/j.seppur.2020.117185.

Al Momani, F. A. & Örmeci, B. 2014 Measurement of polyacrylamide polymers in water and wastewater using an in-line UV–vis spectrophotometer. *Journal of Environmental Chemical Engineering* **2** (2), 765–772. https://doi.org/https://doi.org/10.1016/j.jece.2014.02.015.

Berardinelli, A., Hamrouni, A., Dirè, S., Ceccato, R., Camera-Roda, G., Ragni, L., Palmisano, L. & Parrino, F. 2021 Features and application of coupled cold plasma and photocatalysis processes for decontamination of water. *Chemosphere* **262**, 128336. https://doi.org/https://doi.org/10.1016/j.chemosphere.2020.128336.

Crema, A. P. S., Piazza Borges, L. D., Micke, G. A. & Debacher, N. A. 2020 Degradation of indigo carmine in water induced by non-thermal plasma, ozone and hydrogen peroxide: a comparative study and by-product identification. *Chemosphere* **244**, 125502. https://doi.org/https://doi.org/10.1016/j.chemosphere.2019.125502.

Deng, R., He, Q., Yang, D., Dong, Q., Wu, J., Yang, X. & Chen, Y. 2021 Enhanced synergistic performance of nano-Fe_0-CeO_2 composites for the degradation of diclofenac in DBD plasma. *Chemical Engineering Journal* **406**, 126884. https://doi.org/https://doi.org/10.1016/j.cej.2020.126884.

Farrokhpay, S. & Filippov, L. 2017 Aggregation of nickel laterite ore particles using polyacrylamide homo and copolymers with different charge densities. *Powder Technology* **318**, 206–213. https://doi.org/https://doi.org/10.1016/j.powtec.2017.05.021.

Gilbert, W. J. R., Johnson, S. J., Tsau, J. S., Liang, J. T. & Scurto, A. M. 2017 Enzymatic degradation of polyacrylamide in aqueous solution with peroxidase and H_2O_2. *Journal of Applied Polymer Science* **134** (10). https://doi.org/10.1002/app.44560.

Gong, S., Sun, Y., Zheng, K., Jiang, G., Li, L. & Feng, J. 2020 Degradation of levofloxacin in aqueous solution by non-thermal plasma combined with Ag_3PO_4/activated carbon fibers: mechanism and degradation pathways. *Separation and Purification Technology* **250**, 117264. https://doi.org/https://doi.org/10.1016/j.seppur.2020.117264.

Guo, H., Jiang, N., Wang, H., Shang, K., Lu, N., Li, J. & Wu, Y. 2019 Enhanced catalytic performance of graphene-TiO_2 nanocomposites for synergetic degradation of fluoroquinolone antibiotic in pulsed discharge plasma system. *Applied Catalysis B: Environmental* **248**, 552–566. https://doi.org/https://doi.org/10.1016/j.apcatb.2019.01.052.

Hu, C., Lan, Y., Qu, J., Hu, X. & Wang, A. 2006 Ag/AgBr/TiO_2 visible light photocatalyst for destruction of azodyes and bacteria. *The Journal of Physical Chemistry B* **110** (9), 4066–4072. https://doi.org/10.1021/jp0564400.

Jiang, N., Guo, L., Qiu, C., Zhang, Y., Shang, K., Lu, N., Li, J. & Wu, Y. 2018 Reactive species distribution characteristics and toluene destruction in the three-electrode DBD reactor energized by different pulsed modes. *Chemical Engineering Journal* **350**, 12–19. https://doi.org/https://doi.org/10.1016/j.cej.2018.05.154.

Kim, K.-S., Kam, S. K. & Mok, Y. S. 2015 Elucidation of the degradation pathways of sulfonamide antibiotics in a dielectric barrier discharge plasma system. *Chemical Engineering Journal* **271**, 31–42. https://doi.org/https://doi.org/10.1016/j.cej.2015.02.073.

Lu, M., Wu, X. J. & Wei, X. F. 2012 Chemical degradation of polyacrylamide by advanced oxidation processes. *Environmental Technology* **33** (9), 1021–1028. https://doi.org/10.1080/09593330.2011.606279.

Ma, J. Y., Fu, K., Fu, X., Guan, Q. Q., Ding, L., Shi, J., Zhu, G. C., Zhang, X. X., Zhang, S. H. & Jiang, L. Y. 2017 Flocculation properties and kinetic investigation of polyacrylamide with different cationic monomer content for high turbid water purification. *Separation and Purification Technology* **182**, 134–143. https://doi.org/10.1016/j.seppur.2017.03.048.

Ma, L. L., Hu, T., Liu, Y. C., Liu, J., Wang, Y. Y., Wang, P. Z., Zhou, J. Y., Chen, M. Y., Yang, B. & Li, L. L. 2021 Combination of biochar and immobilized bacteria accelerates polyacrylamide biodegradation in soil by both bio-augmentation and bio-stimulation strategies. *Journal of Hazardous Materials* **405**. https://doi.org/10.1016/j.jhazmat.2020.124086.

Meng, Z., Li, C., Li, M., Li, Q. & Liu, X. 2018 Enhanced photocatalytic degradation of hydrolyzed polyacrylamide by three-dimensional Cu_2O/graphene@nickel foam composite. *Desalination and Water Treatment* **108**, 246–252. https://doi.org/10.5004/dwt.2018.21943.

Qin, C., Guo, M., Zheng, Y., Yu, R., Huang, J., Dang, X. & Yan, D. 2021 Two-component zeolite-alumina system for toluene trapping with subsequent nonthermal plasma mineralization. *Journal of Industrial and Engineering Chemistry* **95**, 215–223. https://doi.org/https://doi.org/10.1016/j.jiec.2020.12.024.

Ren, J., Jiang, N., Shang, K., Lu, N., Li, J. & Wu, Y. 2019 Evaluation of trans-ferulic acid degradation by dielectric barrier discharge plasma combined with ozone in wastewater with different water quality conditions. *Plasma Science and Technology* **21** (2), 025501. https://doi.org/10.1088/2058-6272/aaef65.

Sang, W., Cui, J., Mei, L., Zhang, Q., Li, Y., Li, D., Zhang, W. & Li, Z. 2019 Degradation of liquid phase N,N-dimethylformamide by dielectric barrier discharge plasma: mechanism and degradation pathways. *Chemosphere* **236**, 124401. https://doi.org/https://doi.org/10.1016/j.chemosphere.2019.124401.

Tang, S. F., Yuan, D. L., Li, N., Qi, J. B., Gu, J. M. & Huang, H. M. 2017 Hydrogen peroxide generation during regeneration of granular activated carbon by bipolar pulse dielectric barrier discharge plasma. *Journal of the Taiwan Institute of Chemical Engineers* **78**, 178–184. https://doi.org/10.1016/j.jtice.2017.05.025.

Tang, S., Yuan, D., Rao, Y., Li, N., Qi, J., Cheng, T., Sun, Z., Gu, J. & Huang, H. 2018 Persulfate activation in gas phase surface discharge plasma for synergetic removal of antibiotic in water. *Chemical Engineering Journal* **337**, 446–454. https://doi.org/https://doi.org/10.1016/j.cej.2017.12.117.

Wei, L., Wang, X., Chen, S., Li, Q. & Guo, L. 2018 Study of the influencing factors of sedimentation separation of polymer-contained sewage in gravity sedimentation tank. *Nature Environment and Pollution Technology* **17**, 367–374.

Xu, H., Ma, R., Zhu, Y., Du, M., Zhang, H. & Jiao, Z. 2020 A systematic study of the antimicrobial mechanisms of cold atmospheric-pressure plasma for water disinfection. *Science of The Total Environment* **703**, 134965. https://doi.org/https://doi.org/10.1016/j.scitotenv.2019.134965.

Yin, X. Q., Jing, B., Chen, W. J., Zhang, J., Liu, Q. & Chen, W. 2017 Study on COD removal mechanism and reaction kinetics of oilfield wastewater. *Water Science and Technology* **76** (10), 2655–2663. https://doi.org/10.2166/wst.2017.435.

Zhan, J., Liu, Y., Cheng, W., Zhang, A., Li, R., Li, X., Ognier, S., Cai, S., Yang, C. & Liu, J. 2018 Remediation of soil contaminated by fluorene using needle-plate pulsed corona discharge plasma. *Chemical Engineering Journal* **334**, 2124–2133. https://doi.org/https://doi.org/10.1016/j.cej.2017.11.093.

Zhao, L. M., Cheng, Y., Yin, Z. C., Chen, D. F., Bao, M. T. & Lu, J. R. 2019 Insights into the effect of different levels of crude oil on hydrolyzed polyacrylamide biotransformation in aerobic and anoxic biosystems: bioresource production, enzymatic activity, and microbial function. *Bioresource Technology* **293**. https://doi.org/10.1016/j.biortech.2019.122023.

Zhou, R., Zhou, R., Zhang, X., Tu, S., Yin, Y., Yang, S. & Ye, L. 2016 An efficient bio-adsorbent for the removal of dye: adsorption studies and cold atmospheric plasma regeneration. *Journal of the Taiwan Institute of Chemical Engineers* **68**, 372–378. https://doi.org/https://doi.org/10.1016/j.jtice.2016.09.030.

Zhu, M. J., Yao, J., Qin, Z. H., Lian, L. N. & Zhang, C. 2017 Response surface methodology approach for the optimisation of adsorption of hydrolysed polyacrylamide from polymer-flooding wastewater onto steel slag: a good option of waste mitigation. *Water Science and Technology* **76** (4), 776–784. https://doi.org/10.2166/wst.2017.245.

First received 17 October 2022; accepted in revised form 27 January 2023. Available online 9 February 2023